Mendeleev Commun., 2027, **37**, JUST ACCEPTED

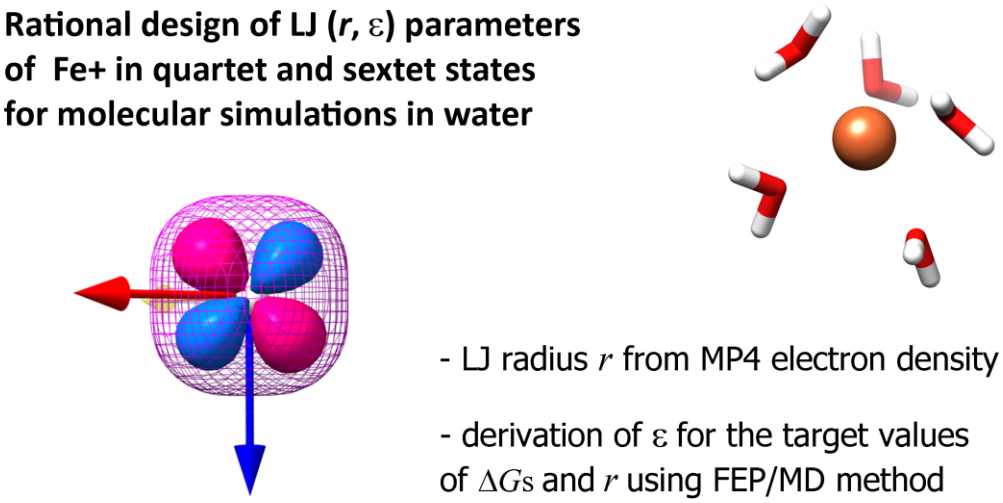
Received 10.07.26 26/8146
Revised 29.09.26

Free energy MD and QM parameterization of the Fe^+ force field in water

Daniil A. Logvinov and Victor B. Luzhkov*

Federal Research Center of Problems of Chemical Physics and Medicinal Chemistry, Russian Academy of Sciences, 142432 Chernogolovka, Moscow Region, Russian Federation.
E-mail: vbl@icp.ac.ru

DOI: 10.71267/mencom.8146



Nonbonded nonpolarizable force field parameters of Fe(I) in water have been determined using microscopic free energy perturbation molecular dynamics (FEP/MD) simulations and correlated MP4 ab initio calculations. The van-der-Waals radii of the Fe^+ ion with electron spin multiplicities M = 4 and 6 were derived from the MP4 electron density calculations and employed in the calibration of the 12–6 Lennard-Jones parameters. The finishing LJ parameters were determined from the FEP/MD calculations of hydration free energies of Fe^+ while the ion coordination numbers were taken for an additional control.

Keywords: Fe(I), nitrosyl iron complexes, molecular dynamics, free energy perturbation, MP4 method.

The iron-sulfur-nitrosyl complexes (ISNCs) with the $Fe(NO)_2$ core group and functional thio ligands are actively studied due to their interesting chemical and biological properties.[1–5] According to the experimental data the iron atom in tetrahedral ISNCs has a formal charge of +1 and electron spin multiplicity $M = 4$.[4] The recent quantum mechanical (QM) calculations at the MP4 level of theory support this type of electronic structure in the hydrate complexes of $Fe(NO)_2$.[6] The individual Fe^+ ion is not registered in water, but its hydrates are observed in gas phase (e.g., citations in ref. 6). Accurate modelling of intermolecular interactions of their core fragment, including determination of the force field (FF) parameters of Fe^+, is of big interest and novelty due to involvement of DNICs in various biochemical reactions.

The microscopic free energy molecular dynamics (MD) and Monte Carlo (MC) simulations with nonpolarizable FF had been broadly employed in the computational studies of thermodynamics of monovalent metal ions in water solution and proteins (e.g., refs. 7–22) and continue to be actively used in molecular modelling. The FF calibration is an important step in the free energy simulations of "metal ion – water" systems. Beginning from the work of Åqvist in 1990[10] parametrization of nonpolarizable FF of metal ions was commonly performed mapping the results of the free energy simulations to experimental data on ion hydration.[10,18–22] In this work we have calibrated the Lennard-Jones (LJ) parameters of the Fe^+ cation from the free energy MD calculations using the target free energy, ΔG_s, of this ion determined in the recent theoretical calculations[6] of the structure–activity relationships.

The FF potential of the nonbonded ion–water interactions, $U_{I–w}$, was calculated as the sum of the van-derWaals and electrostatic interatomic terms according to equation (1)

$$U_{I-w} = \sum_{I,j}^{Npair} \left[\varepsilon_{Ij} \left(\left(\frac{r_{Ij}^m}{r_{Ij}} \right)^{12} - 2 \left(\frac{r_{Ij}^m}{r_{Ij}} \right)^{6} \right) + \frac{q_I q_j}{r_{Ij}} \right] , \quad (1)$$

$$r_{Ij}^m = r_I^m + r_j^m \ , \ \varepsilon_{Ij} = \sqrt{\varepsilon_I \varepsilon_j} \quad . \tag{2}$$

Here, r_{Ij} is the distance between the ion I and water atom j, q_I and q_j are the fixed charges of ion and water atoms. The effective van-der-Waals radii, r_{Ij}^m, and the well depth, ε_{Ij}, are calculated from atomic parameters of iron and water atoms using arithmetic and geometric combination rules, as in Amber FF[13,19-22]. The solvent system included explicit TIP3P[23] water molecules and was treated using spherical boundary conditions with the SCAAS model[9,12]. Water medium beyond the border of the model sphere was considered as polarizable dielectric. More details of calculations are provided in Online Supplementary Materials.

The solvation free energy of Fe^+, $\Delta G_s(Fe^+)$, was calculated using the following equation

$$\Delta G_s\left(Fe^+\right) = -\Delta G\left(Fe^+ \rightarrow d\right) + \Delta G_{Born} \quad . \tag{3}$$

Here, $\Delta G(Fe^+ \rightarrow d)$ is the free energy of ion annihilation in water and ΔG_{Born} is the electrostatic Born energy of ion interaction with the polarizable macroscopic medium outside simulation sphere. The free energies of atom annihilation in equation (3) were calculated by means of the free energy perturbation[24] (FEP) $\Delta G_s(Fe^+)$ and Bennett acceptance ratio[25] (BAR) approaches. Atom annihilation means its transformation to a fictive atom d with zero Lennard-Jones (LJ) parameters and charge. The Born term is given by the expression $\Delta G_{Born} = -\frac{q_I^2}{2r_{mod}}\left(1 - \frac{1}{\varepsilon_w}\right)$, where r_{mod} is the radius of the model water sphere, ε_w is the dielectric constant of water. The discussion of the free energy simulations in the SCAAS water model can be found elsewhere in the literature.[9,10,12,26]

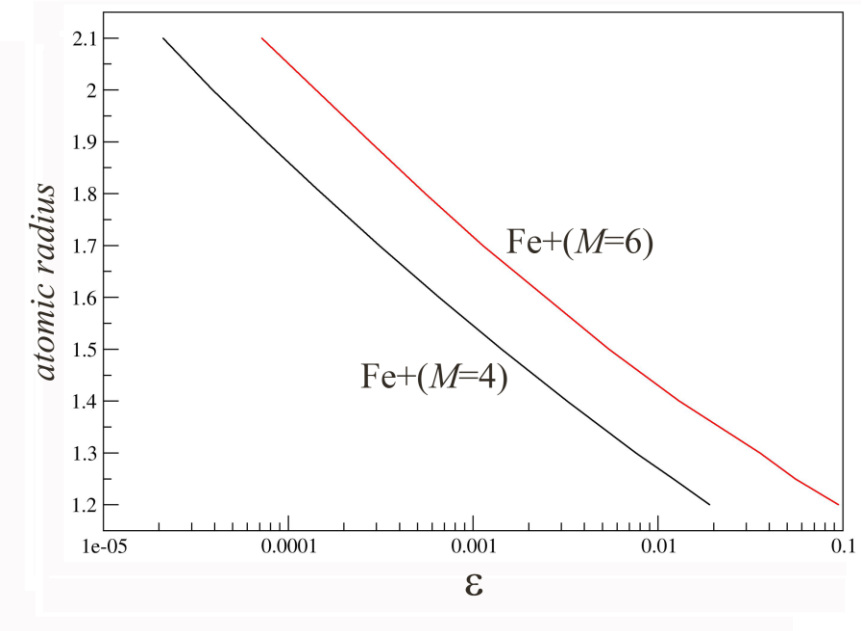


Figure 1 Cross-sections of the hydration free energy surface in the (r_I^m, ε_I^m) coordinates for the target values of ΔG_s(Fe+). Points on the isohydration curves were fitted with the uncertainty of less than 0.1 kcal mol^{-1}. The units for the x and y axes are kcal mol^{-1} and Å.

The r_I^m and ε_I^m ion parameters in the expression for U_{I-w} (1) were varied until the target value of the free energy functional $\Delta G_s(Fe^+)$ in the FEP/MD calculations was attained. The procedure of scanning the $\Delta G_s(Fe^+)$ surface included mutations of $Fe^+ \rightarrow Ne$, as in ref.[10], in which case the ion charge and the LJ parameters were changed simultaneously. The free energy for the Ne→d step was calculated separately and taken as a constant summand in the expression for $\Delta G_s(Fe^+)$. The curve with appropriate (r_I^m, ε_I) pairs is formed by the cross-section of the free energy surface and the plane with the target value of ΔG_s (see Figure 1). The working procedure for building the curves on Fig. 1 involved scan of the ion radius r_I^m within a physically reasonable range and determination of the best fitting ε_I^m value for each r_I^m. Linear interpolation along the free-energy surface was used to trace the best fitting ε_I^m values. Discrete sets of the (r_I^m, ε_I^m) pairs for Fe^+ in two electronic states of (wide infra) were

calculated in this way for r_I^m changing between 1.2 Å and 2.1 Å. The obtained isohydration curves for Fe^+ can be compared to similar graphs for monovalent metal cations.[19–21]

In view of the multiple solutions it is essential to apply additional criteria in order to select single appropriate pair (r_I^m, ε_I^m). The values of the LJ parameters for monovalent metal ions had previously been derived using the target numbers for ΔG_s either in a somewhat ad hoc manner[10,18] or by additionally taking into account the ion–water oxygen distances, water coordination numbers (CN), or the noble gas curves.[19-22]. In the present work we have estimated the r_I^m parameter of Fe^+ from electron density distribution obtained from correlated ab initio QM calculations.

The QM calculations were performed for the Fe^+ ion in the ground $3d^64s^1$ electronic state with electron spin multiplicity $M = 6$ (^6D) and in the excited $3d^7$ state with multiplicity $M = 4$ (^4F) at the MP4/def2-QZVPP level of theory (as in ref.[6]). Full MP4 electron density was considered in the electron density calculations. The boundary of the electron density surface was chosen at the level of 0.001 e $bohr^{-3}$. The electron isodensity surface and the corresponding average atom radius R_{el} were calculated using utility written earlier[27] in the study of fullerene C_{60}.

The obtained electron isodensity surface of Fe^+ in the quartet state ($^4Fe^+$) has a polyhedral shape that is formed by electron densities of the occupied atomic orbitals in the $3d^7$ state (see Figure S1). The points on the external isodensity surface lie at the distance of 1.68 to 1.93 Å from the atom center. The average atomic radius R_{el} of $^4Fe^+$ is 1.81 Å in this case. According to the previous correlated QM calculations[6] the first coordination shell of the $^4Fe^+$ ion comprises from 4 to 6 H_2O and NO ligands in gas phase. The packing of ligands is determined by coordination bonds with $^4Fe^+$ and by ligand–ligand interactions. Four water molecules can be arranged in stable square or tetrahedral configurations around $^4Fe^+$, while four H_2O and two NO ligands form a stable octahedron around $^4Fe^+$.[6] In view of pronounced

plasticity of the coordination shell of $^4Fe^+$ the effective atomic sphere can be considered as a reasonable approximation for the polyhedron shape of this ion. The shape and dimension of the external isodensity surface of Fe^+ in the sextet state ($^6Fe^+$) is determined mainly by the outer occupied 4s atomic orbital and the points on this surface have a much lower variation of the distance from the center, 2.02 – 2.07 Å. The atomic radius R_{el} of $^6Fe^+$ obtained from the MP4 calculations is 2.04 Å which is close to the radius of 2.03 Å from relativistic all-electron density DFT calculations[28].

The proposed (r_I^m, ε_I^m) parameters of Fe^+ and the results of the FEP/MD calculations are given in Table 1. The numbers for r_I^m are taken from electron density calculations, $r_I^m = R_{el}$. The minima of the potential energy, $R'_{I–Ow}$, of the Fe^+–H_2O monohydrate given by eq. (1) are at 2.00 and 2.08 Å for $^4Fe^+$ and $^6Fe^+$ respectively (see Table 1). These distances can be compared to the corresponding positions of minima at 2.02 and 2.06 Å obtained from the correlated QM calculations[6] of these complexes. The first maximum, $R_{I–Ow}$, in the calculated radial distribution functions (RDF) of water oxygen, $g_O(r)$, is located at 2.08 Å for $^4Fe^+$ and at 2.18 Å for $^6Fe^+$ (see Table 1, Figure S2). The first hydration shell measured from zero to the bottom of the first minimum comprises ~5 water molecules for $^4Fe^+$ and about 5 to 6 – for $^6Fe^+$ (see Table 1). In a typical snapshot from the equilibrium MD trajectory the $^4Fe^+$ ion is surrounded by four H_2O molecules arranged in a square motif and the fifth H_2O molecule found in axial position (Figure S3). Generally the atomic radii from QM calculations correlate with the van-der-Waals radii derived from crystal structures.[28] The CN value of the bare $^4Fe^+$ cation from our MD simulations with the derived parameters is ~5 which is close to CN = 4 – 6 from QM calculations[6] of $^4Fe^+$ and hydrated $Fe(NO)_2$ group. The given agreement supports applicability of the electron density based LJ radius r_I^m and the related ε_I^m to modelling of ion – water solution.

Table 1 The LJ parameters,[a] ion–water distances[b] and hydration free energies of the Fe^+ ions from the FEP/MD simulations

Ion	r_I^m	ε_I^m	$R'_{I–Ow}$	$R_{I–Ow}$	$<n_w>$	$\Delta G(Fe^+ \rightarrow Ne)$ [c]	ΔG_s [c]	ΔG_s^{ref} [c]
Fe^+ M=4	1.81	0.000142	2.00	2.08	4.96	112.5±0.2	–121.2±0.2	–121.2±3.8[6]
Fe^+ M=6	2.04	0.000108	2.10	2.18	5.44	104.2±0.2	–112.9±0.2	–112.9±3.8[6]

[a] r_I^m and other distances in Å, ε_I^m and free energies in kcal mol^{-1}, q_I = +1 e.u.; [b] $R'_{I–Ow}$ is the 'ion–water oxygen' distance in the minimum of potential (1) for TIP3P water, $R_{I–Ow}$ – the position of the first maximum of $g_O(r)$, $<n_w>$ – the average number of water molecules in the region from zero to the minimum of the first well of $g_O(r)$; [c] $\Delta G_s(Fe^+) = -\Delta G(Fe^+ \rightarrow Ne) - \Delta G(Ne \rightarrow d) + \Delta G_{Born}$ where $\Delta G_2(Ne \rightarrow d)$ = –2.2±0.1 kcal mol^{-1} and ΔG_{Born}= –10.9 kcal mol^{-1} for a 15Å-water sphere, ΔG_s^{ref} are the target values.

The closure of the thermodynamic cycle in the Fe^+ annihilation was validated from the free energies of a slightly different, $Fe^+ \rightarrow Fe^0$ and $Fe^0 \rightarrow d$, mutation paths (see Table S1). Similar free energy MD simulations were performed for annihilation of the alkali metal ions Na^+ and K^+. The calculated ΔG_s for the considered metal ions M^+ closely follow the results of calculations given in Table 1 and the literature results[6,10] for ΔG_s^{ref} of these ions. Mutation of the ion charge +1 to zero at the $M^+ \rightarrow M^0$ path yields electrostatic polar contribution, ΔG_{pol}, and mutation of the LJ parameters to zero at the $M^0 \rightarrow d$ path – nonpolar contribution, ΔG_{np}, to ΔG_s. The largest contribution and variation in ΔG_s come from the electrostatic term ΔG_{pol} (see Table S1). The results from the accompanying BAR calculations are close to the FEP results (see Table S1).

In conclusion we have derived the nonbonded 12–6 LJ parameters of the Fe^+ ion for nonpolarizable FF given in equation (1). This type of potentials with fixed atomic charges,

Class I, are widely employed in the MD simulations of biomolecular systems (e.g., refs.[29,30]). The neglect of polarization effect in the Class I FFs is partially compensated by the choice of overpolarized partial atomic charges in accompanying water models. Spin effects are not taken into account in such FFs. In our work we discern the Fe^+ cations with different electron spin multiplicities and implicitly account for spin effects in the derived FF by choosing the LJ atomic radii r_I^m from correlated ab initio QM calculations. The obtained LJ atomic parameters of Fe^+ rely on the combination with the TIP3P potential of water. Same atomic radius r_I^m of Fe^+ can possibly be employed in the MD calculations with other water potentials but additional re-calibration of the ε_I values would be required in that case. Transferability of ion potentials between different water potentials and solvent models with different boundary conditions had been discussed elsewhere in the literature.[18–22] The proposed LJ parameters of Fe^+ can also be instrumental in derivation of nonpolarizable FF for ISNCs.

The work was financially supported by the Ministry of Science and Education of the Russian Federation via the FRC PCP MC state theme № 124020500019-2.

Online Supplementary Materials

Supplementary data associated with this article can be found in the online version at doi: 10.71267/mencom.8146

References

1. A. F. Vanin, *Int. J. Mol. Sci.*, 2021, **22**, 10356; https://doi.org/10.3390/ijms221910356.
2. D. R. Truzzi, N. M. Medeiros, O. Augusto and P. C. Ford, *Inorg. Chem.*, 2021, **60**, 15835; https://doi.org/10.1021/acs.inorgchem.1c00823.
3. L. M. Mazina, O. V. Pokidova, V. B. Luzhkov, K. S. Ruina and N. A. Sanina, *Russ. Chem. Bull.*, 2025, **74**, 2190; https://doi.org/10.1007/s11172-025-4703-6.
4. N. A. Sanina, G. I. Kozub, T. A. Kondrat'eva, D. V. Korchagin, G. V. Shilov, R. B. Morgunov, N. S. Ovanesyan, A. V. Kulikov, T. S. Stupina, A. A. Terent'ev and S. M.

Aldoshin, *J. Mol. Struct*., 2022, **1266**, 133506; https://doi.org/10.1016/j.molstruc.2022.133506.

5. V. B. Krapivin and V. B. Luzhkov, *Mendeleev Commun*., 2026. **36**, 382; https://doi.org/10.71267/mencom.7993.
6. D. A. Logvinov and V. B. Luzhkov, *Russ. Chem. Bull.*, 2026, **75**, 1433; https://doi.org/10.1007/s11172-026-4993-3.
7. T. P. Lybrand, I. Ghosh and J. A. McCammon, *J. Am. Chem. Soc.*, 1985, **107**, 7793; https://doi.org/10.1021/ja00311a112.
8. T. P. Straatsma and H. J. C. Berendsen, *J. Chem. Phys.*, 1988, **89**, 5876; https://doi.org/10.1063/1.455539.
9. G. King and A. Warshel, *J. Chem. Phys.*, 1989, **91**, 3647; https://doi.org/10.1063/1.456845.
10. J. Åqvist, *J. Phys. Chem.*, 1990, **94**, 8021; https://doi.org/10.1021/j100384a009.
11. D. Beglov and B. Roux, *J. Chem. Phys.*, 1994, **100**, 9050; https://doi.org/10.1063/1.466711.
12. Y. Y. Sham and A. Warshel, *J. Chem. Phys.*, 1998, **109**, 7940; https://doi.org/10.1063/1.477441.
13. J. Wang and P. A. Kollman, *J. Am. Chem. Soc.*, 1998, **120**, 11106; https://doi.org/10.1021/ja980464l.
14. J. Åqvist and V. Luzhkov, *Nature*, 2000, **404**, 881; https://doi.org/10.1038/35009114.
15. V. B. Luzhkov and J. Åqvist, *Biochim. Biophys. Acta*, 2001, **1548**, 194; https://doi.org/10.1016/S0167-4838(01)00213-8.
16. S. Bernèche and B. Roux, *Nature*, 2001, **414**, 73; https://doi.org/10.1038/35102067.
17. V. B. Luzhkov, M. Almlöf, M. Nervall and J. Åqvist, *Biochemistry*, 2006**, 45,** 10807; https://doi.org/10.1021/bi0610799.

18. K. P. Jensen and W. L. Jorgensen, *J. Chem. Theory Comput.*, 2006, **2**, 1499; https://doi.org/10.1021/ct600252r.
19. I. S. Joung and T. E. Cheatham, III, *J. Phys. Chem. B*, 2008, **112**, 9020; https://doi.org/10.1021/jp8001614.
20. D. Horinek, S.I. Mamatkulov and R.R. Netz, *J. Chem. Phys.*, 2009, **130**, 124507; https://doi.org/10.1063/1.3081142.
21. P. Li, L. F. Song and K.M. Merz, Jr., *J. Chem. Theory Comput.*, 2015, **11**, 1645; https://doi.org/10.1021/ct500918t.
22. A. Sengupta, Z. Li, L. F. Song, P. Li and K. M. Merz, Jr., *J. Chem. Inf. Model.*, 2021, **61**, 869; https://doi.org/10.1021/acs.jcim.0c01390.
23. W. L. Jorgensen, J. Chandrasekhar, J.D. Madura, R.W. Impey and M.L. Klein, *J. Chem. Phys.*, 1983, **79**, 926; https://doi.org/10.1063/1.445869.
24. R. W. Zwanzig, *J. Chem. Phys.*, 1954, **22**, 1420; https://doi.org/10.1063/1.1740409.
25. C. H. Bennett, *J. Comput. Phys.*, 1976, **22**, 245; https://doi.org/10.1016/0021-9991(76)90078-4.
26. Y. N. Vorobjev and J. Hermans, *J. Phys. Chem.*, 1999, **103**, 10234; https://doi.org/10.1021/jp984211q.
27. V. B. Luzhkov, *Russ. Chem. Bull.*, 2014, **63**, 56; https://doi.org/10.1007/s11172-014-0473-2
28. M. Rahm, R. Hoffmann and N.W. Ashcroft, *Chem. Eur. J.*, 2016, **22**, 14625; https://doi.org/10.1002/chem.201602949.
29. K. Vanommeslaeghe, O. Guvench and A. D. MacKerell Jr., *Curr Pharm Des*. 2014, **20**, 3281; https://doi.org/10.2174/13816128113199990600.
30. S. Riniker, *J. Chem. Inf. Model.*, 2018, **58**, 565; https://doi.org/10.1021/acs.jcim.8b00042.

Received: 10th July 2026; Com. 26/8146